Springer

KSME

Journal of Mechanical Science and Technology 31 (8) (2017) 3861~3873
www.springerlink.com/content/1738-494x(Print)/1976-3824(Online)
DOI 10.1007/s12206-017-0731-y

Collaborative optimization of NURBS curve cross-section in a telescopic boom †

Aimin Ji*, Changsheng Chen, Liping Peng, Pin Lv and Xiaodi He

College of Mechanical & Electrical Engineering, Hohai University, Changzhou, 213022, China

(Manuscript Received July 19, 2016; Revised March 22, 2017; Accepted April 27, 2017)

Abstract

To improve the carrying capacity and reduce the weight of telescopic boom structure in a truck crane, a Collaborative optimization (CO) approach was applied to solve the problems of strength, stiffness and local stability in the telescopic boom structure. First, the complex optimization problem of the telescopic boom structure was decomposed into two-level optimizations: the system level and two subsystem levels for strength and local stability. Second, the underside curve of the boom's cross-section was constructed by the Non-uniform rational B-Splines (NURBS) curve. 3D parametric solid model and the parametric finite element analysis model for the strength and the local stability were then established. Third, the mathematical models of the strength and local stability for the subsystem levels, and the system level were optimized, respectively. The adaptive relaxation factor algorithm and the penalty function approach were applied to improve the efficiency of CO. Next, the CO process which integrates the ANSYS package with ISIGHT platform was implemented. The optimal results show that the carrying capacity of the telescopic boom structure can be significantly improved and its weight efficiently is reduced. Finally, with the comparison of the stress values obtained from both the experimental test and the theoretical computation, highly coincident results could be obtained to verify the reliability of CO of a telescopic boom.

Keywords: Adaptive relaxation factor; Collaborative optimization; Experimental testing; NURBS curve; Telescopic boom

1. Introduction

As the telescopic boom is a key part of the wheel crane, a design for booms with light weight and high bearing capacity is important to guarantee the working performance of a wheel crane. Furthermore, the design optimization of a telescopic boom is an effective way to reduce its weight and improve its carrying capacity. The main parameters of a telescopic boom are the boom length, and the shape and the size of its cross-section. The boom length can be determined by crane operation range; therefore, design optimization of a crane boom can be attributed to cross-section optimization [1]. Considering the telescopic boom as a complicated box-like structure welded with sheet steel plates, the design optimization method based on the Finite element analysis (FEA) is generally used. Derlukiewicz and Praybylek [2] built the FEA model of a telescopic jib mounted on a mobile platform to calculate the maximum stress and deflection. Savković et al. [3] analyzed the local stress increases at the contact zone of box-like section telescopic booms of truck cranes by the Finite element method (FEM). The simulated results by FEM were verified by experimental test, and this research work could give guidelines for the optimum design of box-like sections in telescopic booms. In the design of a telescopic boom, the local stability of thin-walled booms is an important factor to affect the carrying capacity and safety of a crane structure. The absence of local stability could cause local buckling of boom structures. Rust and Schweizerhof [4] analyzed the load limit and the local buckling mode of the thin-walled telescopic boom with FEM. Yao et al. [5] investigated the buckling failure reason of all-terrain crane telescopic boom by FEA. The FEA results indicated that the boom strength met the design requirement, but the detailed local model incurred a stress wrinkle. The buckling of the telescopic boom was caused by the change of stress state from continuity to wrinkle. Therefore, the local stability of the thin-walled booms is a critical factor to optimize the design of the telescopic boom section. Until now, the design optimization of a telescopic crane boom has made some progress. Milomir et al. [6] studied the optimal parameters of pentagonal cross-section by using the Lagrange multiplier method and the differential evolution algorithm, respectively. The results showed that the Lagrangian multiplier method could solve the boom optimization problem of initial point close to optimal solution successfully, while the range of available initial points of the differential evolution algorithm was wide. More solutions which satisfy given constrains could be obtained and the research results can provide some useful references for the optimization of the boom. Xu et al. [7] solved the optimal problem of the hexagonal cross-section of

*Corresponding author. Tel.: +86 51985191959, Fax.: +86 51985120010
E-mail address: jam@ustc.edu
† Recommended by Associate Editor Gil Ho Yoon

the telescopic boom based on Particle swarm optimization (PSO). The optimization model was defined with the weight of the telescopic boom as the objective, the strength, stiffness of telescopic boom, the local stability of web plate as the constraint functions. The obtained optimal results showed that the PSO algorithm had several advantages in convergence and accuracy compared to the conventional algorithms. Wang et al. [8] proposed extended time-dependent Reliability-based design optimization (RBDO) for the telescopic boom by taking the strength degradation and the random total working time into account. The optimal design results showed the difference between considering the random total working time and without consideration. Beo et al. [9] analyzed the design optimization problem for the optimum shape of cross-section in the telescopic boom by using ANSYS with FEM. The effectiveness of the optimization process was evaluated by comparing the calculated values of stresses and deformations with those obtained from experimental measurements. However, the above-mentioned studies [6, 8, 9] did not deal with the local stability of thin-walled structures in the telescopic boom, while the work [7] gave the local stability constraint expressions of web plates in explicit form. Generally, for a polygonal (e.g., pentagonal or hexagonal cross-sections), the local stability of the web plate as the constraint condition could be expressed explicitly in analytical form in the design optimization of a telescopic boom, but for a curved boom (e.g., an ovoid boom profile), the local stability of the thin-walled structures could be only described in the implicit form. The value of critical local buckling stress could be obtained by use of FEA. With the development of a truck crane trending to increasingly large load-carrying capacity and high-lifting height, it is a significant consideration in the design to increase the booms' flexural and torsional modulus, and stability against deformation and to decrease the weight. Consequently, important advances have been made in boom design. Some new cross-sectional profiles of the boom were developed from classic rectangle to pentagon, hexagon, nonagon, dodecagon until curved shape. This means that the lower web plate of the boom needs to be folded gradually until to the arc, corresponding to the improvement of resistance to buckling capacity of the web plate [10]. Therefore, the compressed side of the boom section using the curved shape can significantly improve the local anti-buckling capacity, which provides possibility to design a crane boom with high load-carrying capacity and low weight. However, it is a complex optimization problem to consider the strength, stiffness and local stability of the telescopic boom with a curved profile simultaneously: These are the objectives and contributions of this paper.

Collaborative optimization (CO) is a bi-level optimization approach that decomposes the original complex optimization problem into one system level and several subsystem level problems [11, 12]. Each subsystem optimization is independent, while the system level optimization is to coordinate different optimal solutions in each subsystem by introducing consistency constraints among the subsystem levels. The decomposition of CO is quite similar to the division of engineering design. CO is a promising method that has been successfully used in many cases, such as satellite constellation, naval vessels optimization, light weight of vehicles, and internal combustion engine optimization [13-17]. However, the adoption of consistency constraints in system optimization leads to dissatisfaction of the K-T condition and converging difficulty during optimization [18]. To overcome the drawbacks, many researchers improved the CO algorithms. Alexandrov et al. [19] raised a relaxation factor method, where the system level equality constraints were transformed into the inequality ones through a relaxation factor. Therefore, the optimization satisfies the K-T condition. Jeon et al. [20] proposed an algorithm in which the relaxation factor decreased in proportion to the optimization iterations, but the initial relaxation factor and the proportion coefficient were difficult to determine. Fang et al. [21] proposed the asymptotic relaxation method, in which the relaxation factor is determined according to the two stages of the strong and weak coupling constraints, respectively, to solve the optimization problem of the local optimal solution and the optimization accuracy problem. But the consistency of coupling was also difficult to define, which leads to the difficulty of the appropriate relaxation factor. X. Li, H. Li et al. [22-27] developed a method to choose the relaxation factor value according to inconsistent information dynamic states between different subjects. This method could accelerate the speed of optimization convergence. But during the optimization, the dynamic relaxation method still had problems in the relaxation factor oscillation. The inconsistency between the subsystems cannot be reduced gradually, which will increase the CO iteration times, and the efficiency will be low.

We have introduced the application of the CO method into the telescopic boom design of the truck crane. First, the complex problem of the telescopic boom optimization was decomposed into one system level and the relatively tractable and independent subsystem level optimization problems. Second, NURBS curve was used to construct the compressed side shape of the boom cross-section. The 3D parametric solid model of the telescopic boom, the strength, the stiffness and the local stability FEA model were then established, respectively, with the ANSYS software. Third, the CO model of the telescopic boom was established and the Isight code integrated ANSYS FEA was used to implement the CO process and obtain the optimal solution. Finally, the physical model was made according to the optimized structure sizes of the boom and the stresses obtained from both measuring and theoretical calculation were compared.

2. The idea of CO applied in the telescopic boom

CO consists of a bi-level, namely, system level and subsystem level optimization. Each subsystem level executes its own optimization and obtains the local optimal solutions, which satisfies its constraints and minimizes the discrepancy between the subsystem variables and the system level targets.

The system level is to minimize the system objective and coordinate the optimal solutions of subsystems by using consistency constraints. After several iterations between the system and the subsystems, the unified optimal solution is finally obtained. The formulation of standard CO is given as follows.

The system level optimization:

$$\left.\begin{array}{l}\min \ F(\boldsymbol{z}) \\ \text{s.t. } J_i^*(\boldsymbol{z}) = \left\|\boldsymbol{z} - \boldsymbol{x}_i^*\right\|^2 = 0 \\ i = 1,2,...,N\end{array}\right\}, \tag{1}$$

where $\boldsymbol{z}$ is system design vector, $\boldsymbol{x_i}$ is design vector for subsystem i, x_i^* is the optimal $\boldsymbol{x_i}$ and $J_i^*(\boldsymbol{z})$ is the consistency constraint of system level.

The subsystem level optimization:

$$\left.\begin{array}{l}\min \ J_i = \left\|\boldsymbol{x}_i - \boldsymbol{z}^*\right\|^2 \\ \text{s.t. } \boldsymbol{c}_i(\boldsymbol{x}_i) \le 0\end{array}\right\}, \tag{2}$$

where $\boldsymbol{z}^*$ is the expected value of system design vector which is passed from the system level and held constant during the subsystem level optimization, and $\boldsymbol{c_i(x_i)}$ is the constraint function of the subsystem level.

The main difficulty of design optimization for the telescopic boom with the consideration of the strength, stiffness and local stability simultaneously is that the whole optimization design process involves two types of analysis models and methods. Based on the strength and stiffness criteria, the cross-sectional dimensions of telescopic booms are optimized with the overall FEA model. And based on the local stability criterion, those are optimized with the local buckling FEA model. Furthermore, the former method is a static analysis, while the latter is a buckling eigenvalue analysis that needs the former analysis to obtain the cross-section stress value. Therefore, this is a complicated and comprehensive problem. Additionally, there is also a nested optimization. Local buckling analysis needs to run the optimization for half wavelength and the nested optimization is consequently formed when the overall optimization of the boom is done. To solve such a complicated system level optimization problem, the system can be decomposed into a number of tractable subsystems, and the consistency between subsystems is coordinated by the system level, which is the idea of CO. As the calculation model and analysis method of the strength stiffness and the local stability are different, these two parts are optimized, respectively.

Based on the idea of CO, the optimization of a telescopic boom can be decomposed into a two-subsystem optimization: Subsystem 1 is the strength and stiffness optimization, and subsystem 2 is the boom local stability optimization. In the optimization process, subsystem 1 delivers stress state variables to the subsystem 2. In the optimization of subsystem 1, the increase of the carrying capacity is mainly taken into account. In subsystem 2 optimization, the critical stress of local buckling is mainly considered. After the two subsystems are optimized relatively independently, the full use of material carrying capacity of the telescopic boom and its self-weight minimization are achieved. The optimization results of the two subsystems are coordinated in the system level optimization solution. After several iterations, the unified optimal solution is obtained in the end.

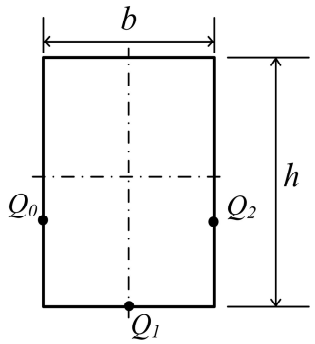

Fig. 1. Cross-section dimensions and the chosen data points.

3. The establishment of telescopic boom analysis model

The model of six-section telescopic boom in a certain truck crane is established as an example and then analyzed. According to the design method of telescopic boom, two working conditions are considered: Condition 1, a whole retraction working condition with a hoist weight of 20 t, a boom length of 6.5 m and an elevation angle of 65°; condition 2, a whole extension working condition with a hoist weight of 1.77 t, a boom length of 25 m and an elevation angle 49.5°. These performance parameter values are provided by the manufacturer.

3.1 The establishment of parametric solid model for telescopic boom

3.1.1 NURBS curve construction for the compressed side in the cross-section of the boom

As the NURBS curve has a fairly good geometric design function, and different kinds of curve shapes can be easily achieved by modifying the control points and weights, it is possible to obtain an optimal cross-sectional shape in the optimization iterative process. So, the widely used cubic NURBS curve [28-30] was employed in this paper to construct the shape for the boom's cross-sectional lower compressed side.

Considering that the height and width of a cross-section are usually determined according to th crane's overall structure during design, we can use a cubic NURBS curve to construct a curve shape for the crane boom compressed side with an assumption that the width b and height h of the boom cross-section are fixed, as shown in Fig. 1. There are mainly four steps: (1) Calculating the node vector with the accumulated

chord length method according to the data points and their weights, then obtaining the basis functions; (2) inversely solving the weights of the control points; (3) inversely solving the control points; and (4) obtaining the NURBS curve function of the boom lower compressed side using basis functions, weights and control points. The detailed process is as follows.

As shown in Fig. 1, three data points, Q_0, Q_1 and Q_2, are taken at the compressed side of the boom cross-section, in which Q_1 is located in the symmetric position of the cross-section. Q_0 and Q_2 are located in the diameter line of the circular arc. The corresponding weights of Q_0, Q_1 and Q_2 are taken as $h_1 = h_2 = h_3 = 1$. The total chord length is [31]

$$d = \sum_{i=1}^{2} |Q_i - Q_{i-1}| = |Q_1 - Q_0| + |Q_2 - Q_1| = 2|Q_1 - Q_0| . \tag{3}$$

The parameter values are:

$$\begin{cases} u_0 = u_1 = u_2 = u_3 = 0 \\ u_4 = u_3 + \dfrac{|Q_1 - Q_0|}{d} = u_3 + 0.5 = 0.5 \\ u_5 = u_6 = u_7 = u_8 = 1 \end{cases} . \tag{4}$$

Therefore, we get the node vector $U = [0, 0, 0, 0, 0.5, 1, 1, 1, 1]$, which is substituted into the Deboor-Cox formula to obtain the basis functions as

$$\begin{cases} N_{i,0}(u) = \begin{cases} 1, & u_i \le u \le u_{i+1} \\ 0, & else \end{cases} \\ N_{i,3}(u) = \dfrac{u - u_i}{u_{i+3} - u_i} N_{i,2}(u) + \dfrac{u_{i+4} - u}{u_{i+4} - u_{i+1}} N_{i+1,2}(u) \end{cases} . \tag{5}$$

The h_0 and h_4 can be calculated, respectively, using h_1, h_2 and h_3, namely,

$$h_0 = \frac{h_2 - h_1}{u_4 - u_3} = 0, \quad h_4 = \frac{h_3 - h_2}{u_5 - u_4} = 0 .$$

Then, inversely solving the weights $\omega_i (i = 0, 1, 2, 3, 4)$ by using following Eq. (6):

$$\begin{bmatrix} l_0 & m_0 & & & \\ l_1 & m_1 & n_1 & & \\ & l_2 & m_2 & n_2 & \\ & & l_3 & m_3 & n_3 \\ & & & l_4 & m_4 \end{bmatrix} \begin{bmatrix} \omega_0 \\ \omega_1 \\ \omega_2 \\ \omega_3 \\ \omega_4 \end{bmatrix} = \begin{bmatrix} h_0 \\ h_1 \\ h_2 \\ h_3 \\ h_4 \end{bmatrix} = \begin{bmatrix} 0 \\ 1 \\ 1 \\ 1 \\ 0 \end{bmatrix} , \tag{6}$$

where $l_0 = -3/\Delta_3$, $m_0 = 3/\Delta_3$, $l_4 = -3/\Delta_4$, $m_4 = 3/\Delta_4$, $l_i = N_{i-1,3}(u_{i+2})$, $m_i = N_{i,3}(u_{i+2})$, $n_i = N_{i+1,3}(u_{i+2}) (i = 1, 2, 3)$, $\Delta_i = u_{i+1} - u_i (i = 3, 4)$.

Using the known data points Q_0, Q_1 and Q_2 and the above mentioned weights, inversely solving the control point

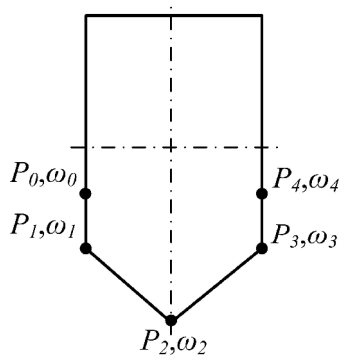

Fig. 2. Weights and control points.

P_i $(i = 0, 1, 2, 3, 4)$ from the following Eq. (7), as shown in Fig. 2.

$$\begin{bmatrix} b_0 & c_0 & & & \\ a_1 & b_1 & c_1 & & \\ & a_2 & b_2 & c_2 & \\ & & a_3 & b_3 & c_3 \\ & & & a_4 & b_4 \end{bmatrix} \begin{bmatrix} P_0 \\ P_1 \\ P_2 \\ P_3 \\ P_4 \end{bmatrix} = \begin{bmatrix} q_0 \\ q_1 \\ q_2 \\ q_3 \\ q_4 \end{bmatrix} , \tag{7}$$

where $b_0 = -3\omega_1/(\omega_0\Delta_3)$, $a_{i+1} = \Delta_{i+3}^2 \omega_i / \left(\Delta_{i+2}^2 \Delta_{i+1}^3\right)$,
$c_0 = 3\omega_1 / (\omega_0\Delta_3)$, $c_{i+1} = \Delta_{i+2}^2 \omega_{i+2} / \left(\Delta_{i+2}^2 \Delta_{i+1}^3\right)$,
$b_{i+1} = \left[1 - \Delta_{i+3}^2 / \left(\Delta_{i+2}^2 \Delta_{i+1}^3\right) - \Delta_{i+2}^2 / \left(\Delta_{i+2}^3 \Delta_{i+2}^2\right)\right] \omega_{i+1} (i = 0, 1, 2)$,
$a_4 = -3\omega_n / (\omega_{n+1}\Delta_{n+1}) = -b_4$, $\Delta_i^k = u_{i+k} - u_i (k = 2, 3)$
$q_i = (a_i + b_i + c_i) Q_{i-1} \quad (i = 1, 2, 3)$.

As Eq. (7) is not sufficient to solve five control points, two conditions need to be added. The tangent vector boundary conditions for the two endpoints are added here as

$$\begin{cases} q_0 = \dfrac{3\omega_1}{\omega_0 (u_4 - u_3)} (P_1 - P_0) \\ q_4 = \dfrac{3\omega_3}{\omega_6 (u_7 - u_6)} (P_6 - P_5) \end{cases} . \tag{8}$$

According to the obtained basis functions $N_{i,3}(u)$, weights ω_i and control points P_i, the NURBS curve function of the boom's sectional lower cover plate can be represented in Eq. (9) [29], as shown in Fig. 3.

$$C(u) = \frac{\sum_{i=0}^{n} N_{i,3}(u) \omega_i P_i}{\sum_{i=0}^{n} N_{1,3}(u) \omega_i} . \tag{9}$$

Since NURBS curve construction for the compressed side in the cross-section of the boom was described above, by continuously moving the position of the data point $Q_0 (Q_2)$, i.e., changing its vertical coordinate, the coordinate of control

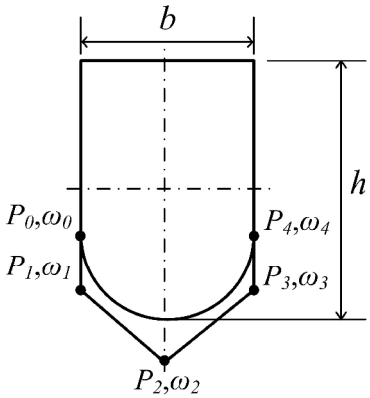

Fig. 3. NURBS curve of the compressed side in the boom section.

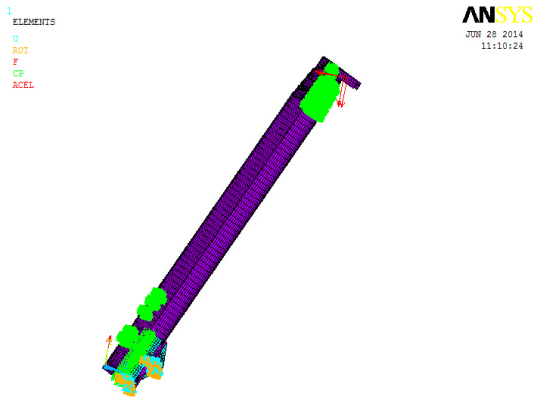

Fig. 4. FEA model of the telescopic boom in the whole retraction condition.

points and corresponding weight factor are obtained in the boom cross-section optimization. Consequently, various NURBS curve cross-sectional shapes are constructed. Finally, the optimum cross-sectional shape that meets performance demands of the boom is obtained.

3.1.2 The establishment of parametric solid model for telescopic boom

First, the mid-face parametric model for the base section is established by the above steps. Second, shapes and sizes of other telescopic sections' mid-surface can be determined according to the space occupied by the telescopic mechanism and sliding pads clearance. To make the subsequent connection setting of different sections and sliding pads convenient and to ensure precision of mesh generation, the shell model of each section is established with a parametric segment. Besides, when building structure models for the base section rear, support of luffing cylinder and head of sixth section, the relationship expressions between these structure sizes and cross-sectional sizes should be built. As the head and rear structure of the boom, structure of support of luffing cylinder are changed and connection maintained with the boom when the cross-sectional size is changed in the optimization. The sliding pad model is established as a solid model by the curved surface where inner and outer booms are in the same place. For two working conditions of the telescopic boom, the whole extension model is established first, and the whole retraction model of boom can then be then obtained by changing the overlap length of sections.

3.2 The establishment of FEA model for telescopic boom

3.2.1 Create FEA model for strength and stiffness

An FEA model of the telescopic boom is created by using ANSYS Shell 63 element for booms and Solid 45 element for sliding pads, respectively. Shell 63 is an elastic element, which is defined by four nodes. It follows Kirchhoff's hypothesis, which is to assume that the normal of the mid-face remains perpendicular to it during bending of the plate. Shell 63 has bending and membrane capabilities. Both in-plane and normal loads are permitted, which conforms to loads of the boom. The node Degrees of freedom (DOF) coupling technology is adopted to simulate the sliding pad contacted between the inner and outer segment of the boom. An identical size in mesh for the sliding pad, the inner and outer segment of the boom in contact zones is set, and therefore the positions of nodes generated in the contact zones coincide with them after mesh. So, the sliding pads, the inner and outer booms and in all the contact zones are connected together by using coincident nodes coupled once, where the normal DOF for the nodes are coupled, and the tangential DOF are released. At first, the hard key points in the loading position of the boom's head should be created to apply conveniently loads acting on the booms. Then the hoisting load, wire rope tension and side load are applied at the hard key points. As for applying the booms' weight and the sliding pads' weight, the value of the gravitational acceleration can be only applied in the direction opposite to gravity. Three directions of translational DOF (UX, UY and UZ) and two directions of rotational DOF (ROTX and ROTY) are constrained at the base section rear end linkage and the luffing cylinder linkage, respectively. The FEA model in the whole retraction condition as an example is shown in Fig. 4. On solving the FEA model, the maximum stress value and deformation value on the telescopic boom obtained are 343 MPa and 15.22 mm, respectively, as shown in Fig. 5.

3.2.2 Create local stability FEA model

The analytical method is adopted in the calculation of local stability of the boom with simple profile shape, such as rectangle. The critical buckling stress can be calculated by means of establishing the FEA model when the boom with curve compressed side of web plate and lower cover plate is encountered. In the FEA of the local stability, the boom' constituent web plate, upper and lower cover plate are all considered. It can solve the difficulty that the critical buckling stress of only a plate is analyzed with the analytical method; accordingly, constraint loads of other disassembled plates are highly difficult to determine. A segment length of the boom as buckling half wave is assumed to build the FEA model. Loads acting on

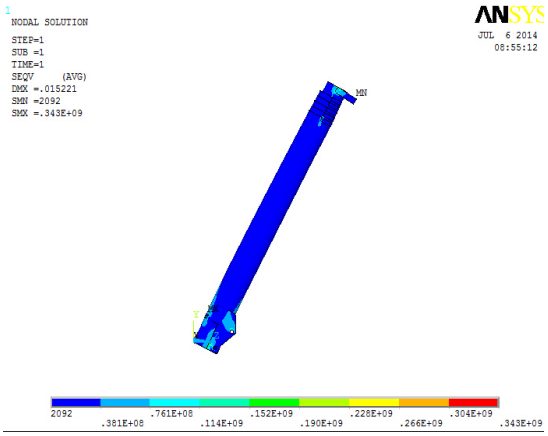

Fig. 5. The stresses distribution of the telescopic boom in the whole retraction condition.

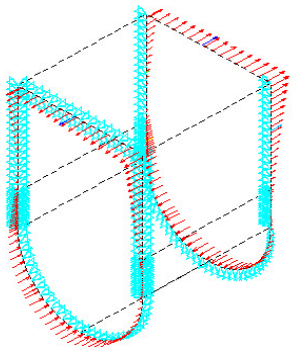

Fig. 6. FEA model on local stability analysis of the boom.

both ends of the model can be applied, taking from the maximum stress distributed value of the boom which is extracted in Sec. 3.2.1. The constraints of two ends on the model are treated to be simply supported [32-34]. Because critical buckling stress reaches the minimum value at the actual half wavelength, the half wavelength is used as a parameter to search for the minimum critical buckling stress by optimization based on the aforementioned FEA. The FEA model is shown in Fig. 6. To be in accordance with the current specification [35], eigenvalue buckling analysis is performed to obtain the critical buckling stress and the buckling mode, shown in Fig. 7.

The foregoing establishment of telescopic boom solid model, FEA model and analysis and calculation are all fulfilled based on the ANSYS software. To invoke and reanalyze the boom model during optimization process, the modeling and analysis process are transformed into ANSYS parametric design language (APDL) command stream text file.

4. The establishment of CO mathematical model of telescopic boom

According to the design method of a telescopic boom, two working conditions, including the whole retraction (base section condition) and the whole extension, need to be considered.

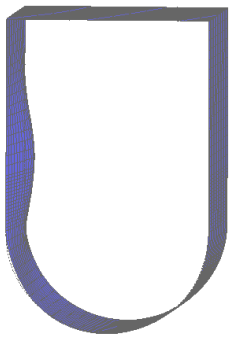

Fig. 7. The local buckling mode of the boom.

The shape and size of base section are determined by the optimization under the whole retraction condition, and the thicknesses of other sections are optimized in the whole extension. Note that when the shape and size of base section's mid-surface are set, shapes and sizes of other telescopic sections can also be determined according to the telescopic mechanism space and sliding pad gap by considering the same profile shape of all sections. Therefore, only the shape and size parameters of the base section's mid-surface can be defined in the following optimization.

4.1 Design variables

The design variables include the width and height of base section's mid-surface, the coordinates of both side data points and thickness of all sections' upper and lower cover plates. W_1 and H_1 represent width and height of the base section, respectively. The vertical coordinate of data point Q_0 (Q_2) is H_{Q1}. R_1 is the thickness of base section upper cover plate, and A_1 is the thickness difference of base section's upper and lower cover plates, so the thickness of the lower cover plate can be represented by (R_1+A_1). As the lower cover plate bears more pressure stress, its thickness is usually no less than that of upper thickness. The number of telescopic sections discussed in this paper is six. For the other five sections, we set their cover plate thickness and thickness differences of sections' upper and lower cover plates as R_2~R_6 and A_2~A_6. We define the sections' thickness as integer design variables.

4.2 Subsystem model 1 of strength and stiffness

The objective of optimization in strength subsystem is to minimize the difference between the design variable of this subsystem and the expected value of system design variable under the constraint condition of stress, deflection and design variables. The mathematical optimization model for the strength and stiffness subsystem in the whole retraction working condition is described as follows:

$$\begin{aligned}\min J_1 = &(R_1^* - R_{11})^2 + (A_1^* - A_{11})^2 + (H_{Q1}^* - H_{Q11})^2 + \\ &+ (H_1^* - H_{11})^2 + (W_1^* - W_{11})^2\end{aligned} \tag{10}$$

$$
\begin{aligned}
s.t.\quad & 114 \le H_{Q11} \le 306, 570 \le H_{11} \le 612, \\
& 370 \le W_{11} \le 404, f \le l^2, \sigma_e \le 484, \\
& R_{11}, R_2, R_3 \in [5,7], R_4, R_5 \in [4,6], R_6 \in [3,5], \\
& A_{11}, A_2, A_3, A_4, A_5, A_6 \in [0,2].
\end{aligned}
$$

where R_1^*, A_1^*, H_{Q1}^*, H_1^* and W_1^* are the optimal solutions of system-level design variables, which are obtained by following system level optimization and delivered to subsystems. R_{11}, A_{11}, H_{Q11}, H_{11} and W_{11} are design variables of subsystem 1 that correspond to the system level R_1, A_1, H_{Q1}, H_1 and W_1. R_2 - R_6 and A_2 - A_6 are local design variables of subsystem 1. The cross-sectional dimensions of the boom are in millimeters. f is a deflection value of the boom. l is the total length of telescopic boom in working condition and its dimension is in meters. σ_e is the von Mises maximum equivalent stress with a unit as MP_a.. The deflection and stress values are obtained by the FEA in Sec. 3.2.1.

4.3 Subsystem model 2 of local stability

The objective of local stability optimization is to minimize the difference between the design variable value of this subsystem and the expected value for system design variable under the condition of meeting the constraint conditions of local critical stress and design variable boundary. The mathematical optimization model of the local stability subsystem in the whole retraction working condition is shown as follows:

$$
\begin{aligned}
\min J_2 = & \left(R_1^* - R_{12}\right)^2 + \left(A_1^* - A_{12}\right)^2 + \left(H_{Q1}^* - H_{Q12}\right)^2 + \\
& \left(H_1^* - H_{12}\right)^2 + \left(W_1^* - W_{12}\right)^2 \\
s.t.\quad & 114 \le H_{Q12} \le 306, 570 \le H_{12} \le 612, \\
& 370 \le W_{12} \le 404, \sigma_{cr} \le 484, \\
& R_{12} \in [5,7], A_{12} \in [0,2].
\end{aligned} \tag{11}
$$

where R_{12}, A_{12}, H_{Q12}, H_{12} and W_{12} are design variables of subsystem 2 that correspond to system level variables R_1, A_1, H_{Q1}, H_1 and W_1. During the optimization of local stability subsystem 2, the buckling critical stress value σ_{cr} is obtained based on the finite element modeling and eigenvalue buckling analysis described in Sec. 3.2.2. The applied load is the stress value on the dangerous section, which is obtained from the calculation of strength and stiffness subsystem and is passed to the local stability subsystem. As shown in Fig. 8, in the subsystem of strength and stiffness, the tensile or compressive stresses S_1~S_9 in the A~I points can be obtained through FEA and passed to the local stability subsystem to perform loading and calculating of the local critical buckling stress.

4.4 System level model

The objective of system optimization is to minimize the booms' total volume (self-weight) to satisfy the constraint condition of design variables consistency. The mathematical optimization model of this system in the whole retraction working condition is shown in Eq. (12):

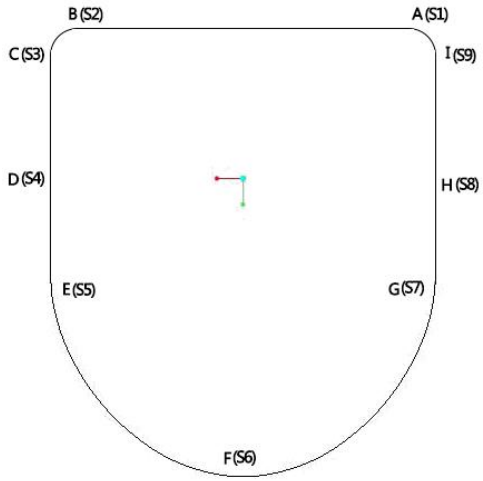

Fig. 8. The extraction position for stress values in the boom section.

$$
\begin{aligned}
& \min V = V_1 + V_2 \\
& s.t.\ \ J_1^* = \left(R_1 - R_{11}^*\right)^2 + \left(A_1 - A_{11}^*\right)^2 + \left(H_{Q1} - H_{Q11}^*\right)^2 + \\
& \qquad \left(H_1 - H_{11}^*\right)^2 + \left(W_1 - W_{11}^*\right)^2 \le s \\
& \qquad J_2^* = \left(R_1 - R_{12}^*\right)^2 + \left(A_1 - A_{12}^*\right)^2 + \left(H_{Q1} - H_{Q12}^*\right)^2 + \\
& \qquad \left(H_1 - H_{12}^*\right)^2 + \left(W_1 - W_{12}^*\right)^2 \le s
\end{aligned} \tag{12}
$$

where V_1 is the volume corresponding to the optimal solution that is derived from strength and stiffness subsystem, V_2 is the volume corresponding to the optimal solution that is obtained from local stability subsystem. J_1^* and J_2^* are the consistency constraint functions between the system level and the two subsystem level design variables, respectively. R_{11}^*, A_{11}^*, H_{Q11}^*, H_{11}^* and W_{11}^* are optimal solutions of design variables in the subsystem 1 optimization, and R_{12}^*, A_{12}^*, H_{Q12}^*, H_{12}^* and W_{12}^* are optimal solutions of design variables in subsystem 2 optimization. These optimal solutions are passed to system level. s is relaxation factor, which is specified as s_1 and s_2, respectively, based on the inconsistency between the system level and subsystems at iterative process according to the following adaptive relaxation algorithm. At the accelerating convergence stage, a penalty function consisting of the system level consistency constraint can be added in the objective function V.

After the base section's dimensions are determined by CO in the whole retraction working condition, the thicknesses of other telescopic sections still need to be calculated in the whole extension working condition. In the whole extension working condition of CO, the system design variables and corresponding design variables of the two subsystems are the upper cover plate thickness and the thickness difference between the upper and lower cover plates for the other telescopic

sections. The mathematical optimization models of the two subsystem levels and the system level are similar to Eqs. (10)-(12), and the design variables need to be replaced in the three equations.

5. The CO method of telescopic boom

As mentioned in the Introduction and Sec. 2, for the conventional CO, the compatibility between the subsystems is ensured by the equality constraints introduced into the system level optimization. However, the equality constraint can cause the system level optimization not to satisfy the K-T condition, and it can result in a hard convergence of optimization. Some CO improvements based on the relaxation factor method have been described in the introduction. However, an appropriate value of relaxation factor is difficult to determine. As the telescopic boom has complex structures, the FEA is used for a performance analysis in each step of the iteration during optimization, which brings large calculations. Thus, it is very urgent to increase the efficiency of CO. Our previous study proposed [36] the adaptive relaxation factor algorithm and penalty function approach based on the inconsistency between system level and subsystem level. In this algorithm, the relaxation factor is adjusted adaptively according to the CO process, and in the final stage of CO, the penalty function is introduced to the system level objective function. With these two approaches, the relaxation factor oscillation and CO efficiency can be improved. Therefore, the adaptive relaxation factor algorithm and the penalty function approach are adopted to solve the CO of telescopic boom.

5.1 The adaptive relaxation factor algorithm

Using s as the relaxation factor, similar to Eq. (1), the consistency constraint between the subsystem i and the system is defined as

$$J_i^*(\boldsymbol{z},\boldsymbol{x}_i^*) = \left\| \boldsymbol{z} - \boldsymbol{x}_i^* \right\|^2 \le s \ . \tag{13}$$

Letting $\boldsymbol{z}^*$ denote the optimal solution vector obtained by the system optimization, then the value of $J_i^*(\boldsymbol{z}^*,\boldsymbol{x}_i^*)$ indicates the optimal solution inconsistency between the subsystem level and the system level. Thus, the degree of the inconsistency k for the two subsystems of telescopic boom can be expressed as

$$k = \sqrt{\left[J_1^*(\boldsymbol{z}^*,\boldsymbol{x}_1^*)\right]^2 + \left[J_2^*(\boldsymbol{z}^*,\boldsymbol{x}_2^*)\right]^2} \ . \tag{14}$$

Considering that the difference between the subsystem optimal solution x_i^* and the system optimal solution $\boldsymbol{z}^*$ is large at the preliminary optimization stage, a large value of the relaxation factor can then be chosen. The relaxation factor s_1 at this stage is defined as

$$s_1 = \lambda^2 \times k, \ \ 0.5 < \lambda < 1 \ . \tag{15}$$

Since λ is a constant less than 1, the inconsistency between the system level and the subsystem level becomes smaller during optimization.

As the CO of telescopic boom proceeds, the inconsistency between system level and subsystem level gradually decreases, and relaxation factor s_1 does the same. While $0.0005 \le s_1 \le 0.005$, to avoid the situation that the oscillation of the relaxation factor leads to the increase of the iteration number and is difficult to converge in CO process, strictly decreasing function can be used to calculate the relaxation factor. Thus, the relaxation factor s_2 at this stage is expressed as

$$s_2 = \{\alpha_i\} \times k, \ \ \alpha_i = 0.25 + \beta / i \ , \tag{16}$$

where $\{\alpha_i\}$ is a decreasing series whose value decreases with the number of iterations, and β is a constant used to control the initial value of s_2.

5.2 The penalty function approach

After the above iteration process of CO, the relaxation factor can be decreased to a small enough value, and the optimal solutions of system level and two subsystems level are very close. At this time, the decreased speed of the inconsistency is slow, only relying on the adjustment of relaxation factor. It means that the convergence rate of CO slows down. To accelerate decreasing of the inconsistency and improving the convergence efficiency, the system consistency constraint is added into the system objective function as the penalty function after $s_1 \le 0.0005$. The penalty function $\varphi(\boldsymbol{z})$ is given by

$$\varphi(\boldsymbol{z}) = \tau \sum_{i=1}^{2} J_i^*(\boldsymbol{z},\boldsymbol{x}_i^*) \ , \tag{17}$$

where τ is a penalty factor. Therefore, the system level objective function is changed from V to $V+\phi(\boldsymbol{z})$.

6. CO realization and optimization results analysis

The optimization models of subsystem 1 for the telescopic boom's strength, stiffness, and subsystem 2 for local stability are established, respectively, based on FEA. Both subsystems perform their own optimization and obtain the respective optimal solutions. The system level coordinates the optimal solutions of the subsystems and finally obtains the unified optimal solutions. The CO process of telescopic boom is illustrated in Fig. 9.

Multidisciplinary design optimization ISIGHT code and integrated ANSYS finite element modeling analysis are used to implement CO process of the telescopic boom. In ISIGHT code, the CO workflow composed of multiple components is set up, which is shown in Fig. 10. In the model, the Simcode components are used to integrate the aforementioned ANSYS

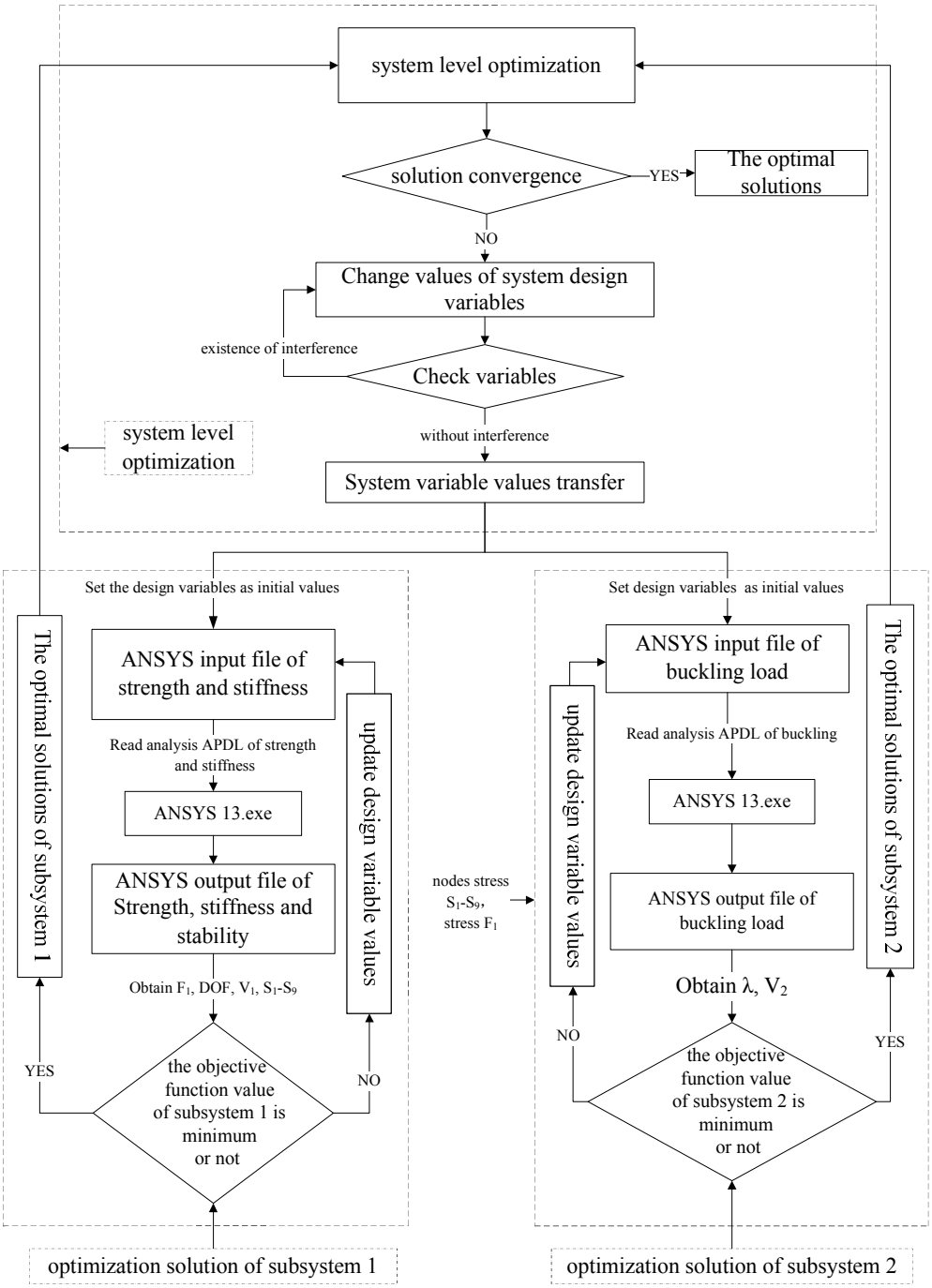

Fig. 9. Architecture of CO for the telescopic boom.

APDL command stream files of FEA for the boom's parametric strength and local stability. Meanwhile, the objective function, constraint conditions, design variables transfer and calculation of relaxation factors are defined, respectively, with multiple calculator components. Considering that the telescopic boom's optimization problem includes real and integer design variables, the Multifunction optimization system tool (MOST) algorithm [37] is used to solve the optimization problems. MOST can handle optimization problems whose design variables are real and integer, and use Sequential quadratic programming (SQP) and branch-and-bound to search for the optimal solutions. Due to the large amount of optimization calculation, HPZ420 workstation is used as a tool. Finally, the system optimal solutions are obtained after several iterations. The iteration result of the minimum boom volume as the objective is shown in Fig. 11. Table 1 gives the comparisons of telescopic boom section dimensions before and after optimization, while Table 2 gives the comparisons of the boom per-

Table 1. Comparison of the optimal design values with the original design values.

Design parameters	H_1	W_1	R_1	R_2	R_3	R_4	R_5	R_6	A_1~A_6
Original design value/mm	612	404	6	6	6	5	5	4	0
Optimized value/mm	598	377	7	5	5	4	4	3	0

Table 2. Comparison of the optimal boom properties with those of the original boom.

Boom performance	Maximum stress /MPa	Deflection /mm	Local buckling critical stress /MPa	Boom volume /mm^3
Before optimization	356	104	193	0.2823×10^9
After optimization	405	105	428	0.2490×10^9

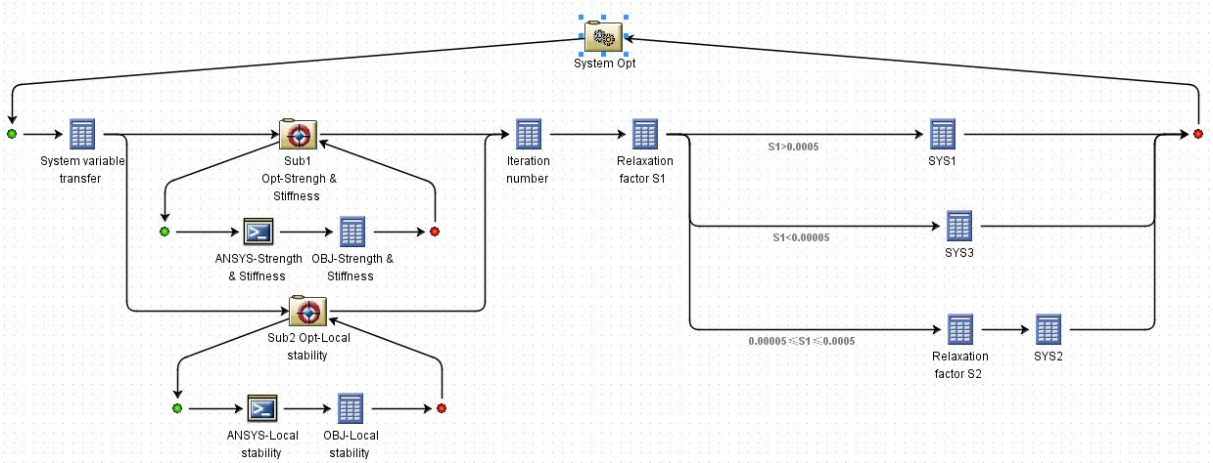

Fig. 10. Integration framework of components of CO in the telescopic boom.

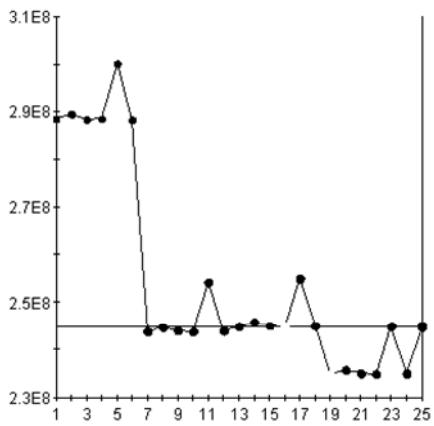

Fig. 11. CO iterative curve of the optimal objective.

formance before and after optimization.

As shown in Tables 1 and 2, the shape of the boom's cross-section becomes more reasonable after optimization. The boom's local buckling critical stress increases from 193 MPa to 428 MPa and its anti-local-buckling ability reaches the same level as the strength, and the maximum load-carrying stress on the boom increases from 356 MPa to 405 MPa. Besides, the thickness of the other sections except for the base section is reduced by 1 mm, which indicates that it takes full

Fig. 12. Measurement system for stresses on the telescopic boom.

advantage of the load-carrying capacity of the material. The total volume of the telescopic boom (self-weight) can be decreased by 11.8 % after optimization.

7. Experimental tests

To check the above optimization results, a physical model for testing was made according to the structure and dimensions of the telescopic boom obtained by optimization. The critical cross-section of the telescopic boom was selected to measure the stress, and the results obtained by experimental testing were then compared with the theoretical calculations. The measuring devices included ASMD2-16 type dynamic strain gauge and DELL notebook computer, the experiment

Table 3. Comparison of the values of measured stress with calculation values in the optimized boom.

Working condition	Section	Test point	Measured value /MPa	Calculation value /MPa	Relative deviation /%
Whole retraction working condition	Base section	1 2 3	-337 -358 -343	-354 -385 -361	5.04 7.54 5.25
Whole extension working condition	Base section	1 2 3	-286 -305 -294	-270 -284 -275	5.59 6.89 6.46
	Sec. 2	1 2 3	-293 -281 -305	-278 -313 -283	5.12 11.39 7.21
	Sec. 3	1 2 3	-251 -308 -264	-273 -295 -284	8.76 4.22 7.58
	Sec. 4	1 2 3	-238 -278 -245	-257 -268 -263	7.98 3.60 7.35
	Sec. 5	1 2 3	-246 -283 -255	-257 -273 -261	4.47 3.53 2.35
	Sec. 6	1 2 3	-218 -232 -212	-204 -256 -228	6.42 10.34 7.55

setup is shown in Fig. 12. ASMD2-16 is a synchronized dynamic strain gauge with high performance to measure various static and dynamic strain of the linear elastic material. In the design and manufacturing of the instrument, the influence factors, such as temperature, humidity, vibration, and static, pulse, electromagnetic radiation, are fully considered. Thus, it has high precision, good linearity, small temperature shift in measurement, and can work safely for a long time. ASMD2-16 can be widely used in complex structural strain testing. The main technical indexes of ASMD2-16 are: 16 channels sampling rate up to 12 kS/s per channel, 0.5 με/0.1 μV resolution ratio, 1.5 με/0.2 μV temperature shift, 5.76 kHz 3 db cut-off frequency, and long wire compensation to remove measuring errors caused by wire resistance. Therefore, ASMD2-16 can meet the needs of boom testing. In the stress testing, data acquisition and processing were conducted by the test software system. To compare the testing results with the optimization results, two working conditions of the whole retraction and the whole extension were employed. The position of the measuring points was selected in the front of luffing cylinder support of the base section at the whole retraction working condition. At the whole extension working condition, the position of the measuring points on the base section was the same as the whole retraction working condition, the positions of the measuring points on the other sections were selected in the vicinity of the overlap with the lower sliding pads, and the layout of three measuring points on the arc surface of the boom is shown in Fig. 13. Considering the impact of the environmental temperature on the measured values of stresses, a temperature compensating strain gauge was then installed in the non-load bearing area, shown in Fig. 14, and the "one to one" compensating mode was applied to the stress value of the measuring point. The comparison between the measured values and the calculation values of the telescopic boom is shown

Fig. 13. Layout of measuring points on the arc surface of the boom.

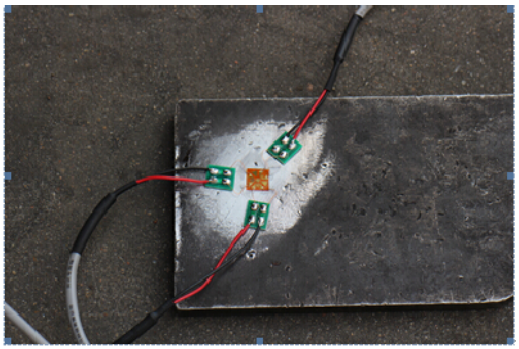

Fig. 14. Temperature compensating strain gauge.

in Table 3. From Table 3, the maximum stress occurs at the measuring point 2, which is located at the lowest point of the lower arc surface for the base section at the whole retraction working condition. The calculation values and measured values reveal compliance. All of the stresses at the critical cross-section do not exceed the allowable stress value, which indicates that the telescopic boom structure after optimization is safe. By comparing the calculation values with the measuring values of stresses, the relative deviation of the both is less than 10 %, except two measuring points, which indicates that the results of optimization with the results of the experimental testing are coincided. The main reason for the result deviation may be that there is inconsistency between the FEA model in optimization and the physical model. For example, when the physical model is made, it is difficult to construct the exact NURBS smooth curve for the boom cross-section, which can only be formed by subsection. In addition, in finite element modeling, the connection between the sliding pad and the boom is the ideal state without gap, but in fact they are loaded and a gap exists. Therefore, error exists between load in the finite element model and the actual model of the boom.

8. Conclusions

The optimization design for a telescopic boom, including complicated comprehensive optimization problems such as strength, stiffness and local stability, is difficult to be solved with conventional optimization methods. Therefore, we decomposed the complicated telescopic boom optimization problem into two more tractable subsystem-level optimization problems of strength and local stability with CO thought. By building the optimization models of system-level and subsystem-level, the CO problem was solved and the uniform optimal solution was obtained in this study. The comparison results between the measured stresses in the physical model and the theoretical calculation show that the optimized design of telescopic boom are reliable.

In the future, we will investigate promoting the efficiency of the CO of telescopic boom with an approximation model. Because the FEA for the telescopic boom costs long time for each optimization iteration, the approximation model is considered as another solution to replace it. However, the accuracy of the approximation model depends on the number of sample points, so how to construct an efficient approximation model for the FEA is one of most important breakthroughs in the future work.

Acknowledgments

The authors would like to acknowledge the funding supported by the National Natural Science Foundation of China (Grant No. 51175146), the Fundamental Research Funds for the Central Universities (Grant No 2012B14014) and the Natural Science Foundation of Jiangsu Province (Grants No BK20160286).

Nomenclature

b	: Width of the boom cross-section
$\boldsymbol{c}_i(\boldsymbol{x}_i)$	: Constraint function of subsystem level
d	: Total Chord length
f	: Deflection value of the boom
h	: Height of the boom cross-section
$J_i^*(\boldsymbol{z})$	: Consistency constraint of system level
P_i	: Control point
Q_0, Q_1, Q_2	: Data points
s	: Relaxation factor
U	: Node vector
$\boldsymbol{x_i}$	: Design vector for subsystem i
x_i^*	: Optimal x_i
$\boldsymbol{z}$	: System design vector
$\boldsymbol{z}^*$	: Expected value of system design vector
ω_i	: Weights
σ_e	: Von Mises maximum equivalent stress

References

[1] Z. Nowak and W. Pogorzelski, Algorithm for the minimum weight design of a telescopic jib, *Computers and Structures*, 8 (1) (1978) 61-65.

[2] D. Derlukiewicz and G. Praybylek, Chosen aspects of FEM strength analysis of telescopic jib mounted on mobile platform, *Automation in Construction*, 17 (2008) 278-283.

[3] M. Savković et al., Stress analysis in contact zone between the segments of telescopic booms of hydraulic truck cranes, *Thin-Walled Structures*, 85 (2014) 332-340.

[4] W. Rust and K. Schweizerhof, Finite element limit load analysis of thin-walled structure by ANSYS (implicit), LS-DYNA (explicit) and in combination, *Thin-Walled Structures*, 41 (2003) 227-244.

[5] J. Yao et al., Buckling failure analysis of all-terrain crane telescopic boom section, *Engineering Failure Analysis*, 57 (2015) 105-117.

[6] M. Gašić et al., Optimization of a pentagonal cross section of the truck crane boom using Lagrange's multipliers and differential evolution algorithm, *Meccanica*, 46 (2011) 845-853.

[7] G. Xu, X. Hou and Q. Dong, Based on the particle swarm optimization of truck crane telescopic jib optimization and implementation, *Frontiers of Manufacturing Science and Measuring Technology III, Applied Mechanics and Materials*, 401-403 (2013) 548-553.

[8] Z. Wang et al., Reliability-based design optimization for box-booms considering strength degradation and random total working time, *J. of Mechanical Science and Technology*, 26 (7) (2012) 2045-2049.

[9] P. Beo, D. Kozak and P. Konjati, Optimization of thin-walled constructions in CAE system ANSYS, *Tehnicki Vjesnik*, 21 (5) (2014) 1051-1055.

[10] U. Hamme and J. Henkel, Neue konzepte im leichtbau-innovativer teleskopausleger eines mobilkrans, *Stahlbau*, 82 (4) (2013) 246-249.

[11] I. Kroo et al., Multidisciplinary optimization methods for aircraft preliminary design, *AIAA*-94-1325.
[12] F. Xiong et al., A moment-matching robust collaborative optimization method, *J. of Mechanical Science and Technology*, 28 (4) (2014) 1365-1372.
[13] B. Roth and I. Kroo, Enhanced collaborative optimization: Application to an analytic test problem and aircraft design, *12th AIAA/ISSMO Multidisciplinary Analysis and Optimization Conference*, AIAA 2008-5841.
[14] I. Budianto and J. Olds, Design and Deployment of a satellite constellation using collaborative optimization, *J. of Spacecraft and Rockets*, 41 (6) (2004) 956-963.
[15] T. Dylan and C. Matthew, A goal-programming enhanced collaborative optimization approach to reducing lifecyle costs for naval vessels, *Structural and Multidisciplinary Optimization*, 53 (2016) 1261-1275.
[16] V. Ganesan, J. Rodriguez and R. Johnston, Collaborative design optimization for light weight design, *SAE 2014 World Congress and Exhibition*, Detroit, MI, United States (2014) 2014-1-0392.
[17] C. McAllister and T. Simpson, Multidisciplinary robust design optimization of an internal combustion engine, *J. of Mechanical Design*, 125 (1) (2003) 124-130.
[18] R. Braun et al., *Implementation and performance issues in collaborative optimization*, AIAA-96-4017.
[19] N. M. Alexandrov and R. M. Lewis, Analytical and computational aspects of collaborative optimization for multidisciplinary design, *AIAA J.*, 40 (2) (2002) 301-309.
[20] K.-S. Jeon, J.-W. Lee and J.-H. Choi, *Efficient system optimization techniques through subspace decomposition and response surface refinement*, AIAA-2002-0321.
[21] P. Fang et al., Asymptotic relaxation based on collaborative optimization, *J. of Shanghai Jiaotong University*, 47 (12) (2013) 1896-1901, 1906 (in Chinese).
[22] X. Li, W. Li and C. Liu, Geometric analysis of collaborative optimization, *Structural and Multidisciplinary Optimization*, 35 (4) (2008) 301-313.
[23] X. Li et al., An alternative formulation of collaborative optimization based on geometric analysis, *ASME J. of Mechanical Design*, 133 (5) (2011) 051005 (1-11).
[24] X. Li et al., Application of collaborative optimization to optimal control problems, *AIAA J.*, 51 (3) (2013) 745-750.
[25] H. Li, M. Ma and W. Zhang, Improving collaborative optimization for MDO problems with multi-objective subsystems, *Structural and Multidisciplinary Optimization*, 49 (2014) 609-620.
[26] H. Li, M. Ma and Y. Jing, A new method based on LPP and NSGA-II for multiobjective robust collaborative optimization, *J. of Mechanical Science and Technology*, 25 (5) (2011) 1071-1079.
[27] H. Li, M. Ma and W. Zhang, Multi-objective collaborative optimization using linear physical programming with dynamic weight, *J. of Mechanical Science and Technology*, 30 (2) (2016) 763-770.
[28] M. Liu et al., Development and implementation of a NURBS interpolator with smooth feedrate scheduling for CNC machine tools, *International J. of Machine Tools and Manufacture*, 87 (2014) 1-15.
[29] R. Saravanan, S. Ramabalan and C. Balamurugan, Multiobjective trajectory planner for industrial robots with payload constraints, *Robotica*, 26 (6) (2008) 753-765.
[30] J. Rakowski and P. Wielentejczyk, Application of the difference equation method to the vibrations analysis of infinite Rayleigh beams by the isogeometric approach, *Archives of Civil and Mechanical Engineering*, 15 (4) (2015) 1108-1117.
[31] L. Piegl and W. Tiller, *The NURBS Book*, 2nd ed., New York: Springer (2010).
[32] A. Ji et al., Finite element analysis for local stability of thin-walled box section, *2008 Asia Simulation Conference-7th International Conference on System Simulation and Scientific Computing,* IEEE Catalog Number: CFP0858D-CDR: 542-546 (2008).
[33] M. Ozakca, N. Taysi and F. Kolcu, Buckling analysis and shape optimization of elastic variable thickness circular and annular plates-I Finite element formulation, *Engineering Structures*, 25 (2003) 181-192.
[34] M. Ozakca, N. Taysi and F. Kolcu, Buckling analysis and shape optimization of elastic variable thickness circular and annular plates-II Shape optimization, *Engineering Structures*, 25 (2003) 193-199.
[35] Chinese National Standards Committee, *GB/T 3811-2008 Design rules for cranes*, Beijing: China Standard Press (2008) (in Chinese).
[36] A. Ji, X. Yin and M. Yuan, Hybrid collaborative optimization based on selection strategy of initial point and adaptive relaxation, *J. of Mechanical Science and Technology*, 29 (9) (2015) 3841-3854.
[37] W. H. Wang, C. H. Tseng and C. B. Tsay, On the optimization of spatial cam mechanisms considering mechanical errors, *International J. of Modelling and Simulation*, 19 (1) (1990) 94-100.

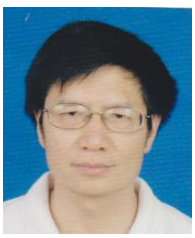

Aimin Ji is a Professor of the College of Mechanical and Electrical Engineering, Hohai University, China. His research interests include digital design and manufacturing, CAD/CAE integration, and multidisciplinary design optimization.